On the MIMO Channel Capacity of Multidimensional Signal Sets

Soon Xin Ng, *Member, IEEE*, and Lajos Hanzo, *Fellow, IEEE*

***Abstract*—In this contribution, the capacity of multiple-input multiple-output (MIMO) systems using multidimensional phase-shift keying/quadratic-amplitude modulation signal sets is evaluated. It was shown that transmit diversity is capable of narrowing the gap between the capacity of the Rayleigh-fading channel and that of the additive white Gaussian noise channel. However, because this gap becomes narrower when the receiver diversity order is increased, for higher order receiver diversity, the performance advantage of transmit diversity diminishes. A MIMO system having full multiplexing gain has a higher achievable throughput than the corresponding MIMO system designed for full diversity gain, although this is attained at the cost of a higher complexity and a higher signal-to-noise ratio. The tradeoffs between diversity gain, multiplexing gain, complexity, and bandwidth are studied.**

***Index Terms*—Capacity, diversity, multiple-input multiple-output (MIMO), multiplexing.**

I. Introduction

THE CAPACITY C of a single-input–single-output (SISO) additive white Gaussian noise (AWGN) channel was quantified by Shannon in 1948 [1], [2]. Since then, substantial research efforts have been invested in finding channel codes that would produce an arbitrarily low probability of error at a transmission rate close to $C^* = C/T$, where T is the symbol period. We note, however, that Shannon's channel capacity is only defined for continuous-input continuous-output memoryless channels (CCMC) [3], where the channel input is a continuous-amplitude discrete-time Gaussian-distributed signal and the capacity is only restricted by either the signaling energy or the bandwidth. Therefore, we will refer to the capacity of the CCMC as the unrestricted bound.

By contrast, in the context of discrete-amplitude quadratic-amplitude modulation (QAM) [4] and phase-shift keying (PSK) [3] signals, we encounter a discrete-input continuous-output memoryless channel (DCMC) [3]. Therefore, the capacity of the DCMC is more pertinent in the design of channel-coded modulation schemes. With the advent of powerful space–time coding schemes [5]–[7], the multiple-input multiple-output (MIMO) channel capacity is of immediate interest. Note that multiple antennas can be utilized for providing diversity gain and/or multiplexing gain [8]. Specifically, space–time trellis coding (STTC) [5] and space–time block coding (STBC) [6], [9] were designed for achieving diversity gains by conveying the same information through different paths over the MIMO channel in order to combat the channel-induced fading. By contrast, Bell Lab's layered space–time (BLAST) [7] scheme transmits independent information in parallel over the MIMO channel for the sake of achieving multiplexing gain, hence increasing the attainable transmission rate. Furthermore, both STTC and STBC schemes are capable of achieving full transmit diversity[1] at the cost of providing no multiplexing gain, whereas the BLAST scheme was designed for achieving full multiplexing gain at the cost of having no transmit diversity gain. The tradeoffs associated with having partial diversity gain and partial multiplexing gain when communicating over MIMO channels was studied in [8].

Note, however, that the STTC scheme [5] is also capable of achieving temporal or time diversity gain, which is commonly referred to as coding gain. On the other hand, the BLAST scheme [7] is unable to provide spatial diversity or temporal diversity, because both of these have been utilized for achieving full multiplexing gain. The STTC scheme may be viewed as a rate-$1/N_t$ channel code, where N_t is the number of transmit antennas. By contrast, the BLAST scheme [7] may be viewed as a rate-1 channel code. Despite having different code rates, both the STTC and BLAST schemes share the same MIMO channel capacity. This is similar to the case where two different-rate temporal domain channel codes share the same M-ary QAM SISO channel capacity when transmitting M-ary QAM signals across the SISO channels. By contrast, the orthogonal STBC may be viewed as a rate-$1/N_t$ spatial-domain repetition coding scheme. The STBC scheme may also be viewed as an MIMO system that employs an orthogonal spreading code in the spatial and temporal domains [10]. Note that the STBC scheme is unable to provide temporal diversity gain because of employing an orthogonal code. Hence, the capacity of the "spatial-domain-spread" STBC MIMO scheme is lower than that of the spread MIMO scheme. Nonetheless, the code orthogonality of the STBC scheme facilitates a low-complexity "despreading" detection compared to the high-complexity maximum likelihood (ML) detection employed by the STTC scheme. The BLAST scheme also achieves its best performance when ML detection is invoked.

However, the MIMO channel's capacity was only found for the CCMC in [11]–[15]. Furthermore, only the SISO AWGN channel capacity was found for multidimensional signal sets,

Manuscript received November 16, 2004; revised April 18, 2005, June 2, 2005, and September 30, 2005. This work was supported by EPSRC, Swindon, U.K., and the EU under the auspices of the Phoenix, Newcom, and Nexway projects. The review of this paper was coordinated by Prof. R. Heath.

The authors are with the School of Electronics and Computer Science, University of Southampton, Southampton SO17 1BJ, U.K. (e-mail: sxn@ecs.soton.ac.uk; lh@ecs.soton.ac.uk).

Digital Object Identifier 10.1109/TVT.2005.863357

[1] A system is said to have a full transmit diversity when the transmit diversity order is identical to the number of transmit antennas [6].

such as M-ary orthogonal signaling [3] and L-ary PSK-based L-orthogonal signaling [16], [17]. More specifically, the L-orthogonal PSK signal [17], [18] is a hybrid form of M-ary orthogonal and PSK signaling, combining the benefits of power-efficient and error-resilient M-ary orthogonal signaling [3, p. 284] as well as bandwidth-efficient PSK signaling. At this stage, we note that STTC and STBC schemes have so far been exclusively designed for complex-valued two-dimensional (2-D) PSK/QAM signal sets but not for multidimensional signal sets. Against this background, the novel contribution of this treatise is the fact that we derive channel capacity formulas applicable to MIMO systems employing multidimensional signal sets in the quest for more error-resilient, power-efficient, and bandwidth-efficient MIMO channel coding schemes.

This paper is organized as follows. In Section II, the multidimensional signal set is described. In Sections III and IV, the channel capacity formulas are derived for the specific orthogonal STBC-based MIMO system and the general MIMO system, respectively. In Section V, the capacity and bandwidth efficiency of the MIMO channel is investigated. Finally, conclusions are offered in Section VI.

II. Multidimensional Signal Set

The dimensionality of a time- and bandlimited signal is defined as [19, pp. 348–351]

$$D = 2WT \tag{1}$$

where W is the bandwidth, and T is the signaling period of the finite-energy signaling waveform. In an L-orthogonal PSK signal set [16], [17], there are $V = WT$ independent L-ary PSK subsets. The total number of waveforms is $M = VL$, and the number of dimensions is $D = 2V$, which is independent of L. Specifically, an L-orthogonal PSK signal requires splitting the original PSK symbol period into V number of proportionately shortened PSK symbol periods and, hence, necessitates V times the bandwidth of PSK signaling in order to transmit $\log_2(M)$ bits. The vector representation of L-orthogonal PSK signaling may be formulated as

$$\mathbf{x}_m = \mathbf{x}_l^{\mathrm{LPSK}} \phi_k, \qquad m = 1, \ldots, M \tag{2}$$

where $l = ((m-1)\%L) + 1$ and $a\%b$ is the remainder of a/b, while $k = (\lfloor (m-1)/L \rfloor + 1)$ and $\mathbf{x}_l^{\mathrm{LPSK}}$ is the classic 2-D L-ary PSK signal. Furthermore, the orthonormal basis function $\phi_k = (\phi_k[1], \ldots, \phi_k[v], \ldots, \phi_k[V])$ is a vector of V elements, which may be constructed from nonoverlapping signaling pulses given as follows:

$$\phi_k[i] = \begin{cases} 1, & i = k \\ 0, & i \neq k \end{cases}. \tag{3}$$

Fig. 1 illustrates an example of $L = 8$-orthogonal PSK signaling, splitting the original signaling interval into $V = 2$ subintervals at the cost of doubling the required bandwidth. The total number of waveforms is $M = VL = 16$, and the number of dimensions is $D = 2V = 4$. Note that only one of the $V = 2$ timeslots of duration T_p is active during the symbol period of $T_s = VT_p$. Therefore, L-orthogonal PSK signaling achieves $\log_2(V)$ bits higher capacity at the cost of V times lower bandwidth efficiency than that of classic L-ary PSK signaling. As we can see in Fig. 1, there are V subsets of L phasors, and each subset is assigned to one of the V orthonormal basis functions ϕ_k. Hence, each subset of phasors is orthogonal to each other. However, the L phasors assigned to the same ϕ_k behave the same way as in ordinary L-ary PSK signaling. Hence, L-orthogonal PSK signaling constitutes a hybrid form of M-ary orthogonal signaling and PSK signaling. For $V = 1$, L-orthogonal PSK signaling represents classic 2-D L-ary PSK signaling. As a further contribution to the current state of the art, we extended the concept of L-orthogonal PSK signaling to L-orthogonal QAM signaling, and we will quantify the achievable capacity of L-orthogonal QAM in Figs. 3–8.

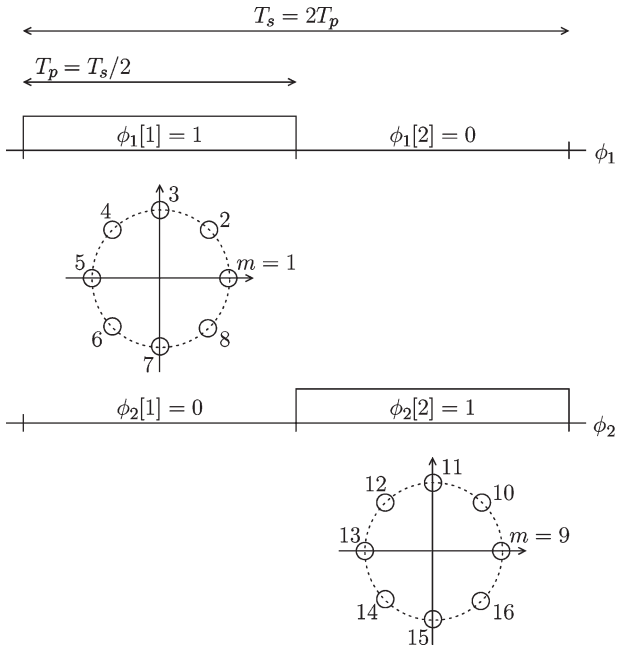

Fig. 1. L-orthogonal PSK example conveying 4 b/symbol using $L = 8$-ary PSK subset, where the total symbol period T_s consists of $V = 2$ LPSK subset's signaling durations T_p.

To elaborate a little further, the $D = 2V$-dimensional L-orthogonal PSK/QAM scheme conveys $\log_2(M)$ bits using V timeslots and orthogonal transmissions, where the total throughput is $\log_2(M)/V$ bits per timeslot. Hence, a V-fold bandwidth expansion occurred compared to the $D = 2$-D PSK/QAM scheme, which conveys $\log_2(M)$ bits per timeslot. However, if a $2V$-dimensional PSK/QAM scheme conveys $V \log_2(M)$ bits using V timeslots, then the total throughput will be $V \log_2(M)/V = \log_2(M)$ bits per timeslot, which is similar to that of the 2-D PSK/QAM scheme. Hence, there is no bandwidth expansion. The multidimensional lattice code [20] belongs to the family of nonorthogonal multidimensional PSK/QAM schemes, where an effective throughput of $\log_2(M)$ bits per timeslot is attained regardless of the signal dimensionality of $D = 2V$. Hence, the bits-per-second-per-hertz bandwidth efficiency of the nonorthogonal multidimensional PSK/QAM scheme is the same as that of the 2-D PSK/QAM scheme when communicating over SISO or MIMO channels. Therefore, the

capacity of the nonorthogonal multidimensional PSK/QAM scheme is simply V times the bandwidth efficiency of the 2-D PSK/QAM scheme. For this reason, in this paper, we mainly focus our attention on the capacity of the multidimensional L-orthogonal PSK/QAM scheme. Note, however, that the orthogonality of the L-orthogonal PSK/QAM scheme is not exploited for achieving diversity or multiplexing gain but only for attaining higher error resilience in a fashion similar to that of the classic M-ary orthogonal scheme [21].

III. Specific MIMO Channel Capacity of the Orthogonal STBC System

When classic $D = 2$-D PSK/QAM is employed, the received signal at receiver i of Alamouti's orthogonal STBC [6] having $N_t = 2$ transmit antennas and N_r receive antennas can be transformed into [22]

$$\mathbf{y}_i = \sum_{j=1}^{N_t} |\mathbf{h}_{i,j}|^2 \mathbf{x} + \mathbf{\Omega}_i = \chi^2_{2N_t,i}\mathbf{x} + \mathbf{\Omega}_i, \qquad i = \{1, \ldots, N_r\} \tag{4}$$

where we define $\vec{\mathbf{y}} = (\mathbf{y}_1, \ldots, \mathbf{y}_{N_r})^T$ as the N_r-element complex-valued received signal vector. Furthermore, $\mathbf{x}$ is the complex-valued transmitted signal; $\mathbf{h}_{i,j}$ is the complex-valued Rayleigh-fading coefficient between transmitter j and receiver i; $\chi^2_{2N_t,i} = \sum_{j=1}^{N_t} |\mathbf{h}_{i,j}|^2$ represents the chi-squared distributed random variable having $2N_t$ degrees of freedom at receiver i; and $\mathbf{\Omega}_i$ is the ith receiver's complex-valued AWGN after transformation, which has a zero mean and a variance of $\chi^2_{2N_t,i}N_0/2$ per dimension, where $N_0/2$ is the original noise variance per dimension. More specifically, because of the code orthogonality of STBC, the MIMO channel was transformed into a single-input–multiple-output (SIMO) channel, where the equivalent Rayleigh-fading coefficient between the transmitter and the ith receiver is given by $\chi^2_{2N_t,i}$, and the equivalent noise at the ith receiver is given by $\mathbf{\Omega}_i$.

It was shown in [23] that a full-rate full-diversity orthogonal STBC also exists for $N_t > 2$. Let us now generalize (4) for each component of a $D >$ 2-D L-orthogonal PSK/QAM scheme as

$$y_i[d] = \chi^2_{2N_t,i}[d]x[d] + \Omega_i[d] \tag{5}$$

where $\mathbf{y}_i = (y_i[1], \ldots, y_i[D])$, $\mathbf{x} = (x[1], \ldots, x[D])$, and $\mathbf{\Omega}_i = (\Omega_i[1], \ldots, \Omega_i[D])$. Note that when $D > 2$, we have $D/2$ number of different $\chi^2_{2N_t,i}$ values for the D-dimensional signals. Specifically, we have $\chi^2_{2N_t,i}[k] = \chi^2_{2N_t,i}[k+1]$ for $k \in \{1, 3, 5 \ldots\}$, because a complex channel has two dimensions. Furthermore, $\Omega_i[d]$ has a variance of $\chi^2_{2N_t,i}[d]N_0/2$ for every D dimensions.

The conditional probability of receiving a D-dimensional signal vector $\vec{\mathbf{y}}$, given that a D-dimensional M-ary signal $\mathbf{x}_m$, $m \in \{1, \ldots, M\}$, was transmitted over an AWGN channel, is determined by the probability density function (PDF) of the noise, yielding

$$p(\vec{\mathbf{y}}|\mathbf{x}_m) = \prod_{d=1}^{D} \frac{1}{\sqrt{\pi N_0}} \exp\left(\sum_{i=1}^{N_r} \frac{-\left(y_i[d] - x_m[d]\right)^2}{N_0} \right) \tag{6}$$

where $N_0/2$ is the channel's noise variance. For the orthogonal STBC MIMO system of (5), we have

$$p(\vec{\mathbf{y}}|\mathbf{x}_m) = \frac{1}{\prod_{d=1}^{D} \sqrt{\pi N_0 \sum_{i=1}^{N_r} \chi^2_{2N_t,i}[d]}} \cdot \exp\left(\sum_{d=1}^{D} \sum_{i=1}^{N_r} \frac{-(y_i[d] - \chi^2_{2N_t,i}[d]x_m[d])^2}{\chi^2_{2N_t,i}[d]N_0} \right). \tag{7}$$

The channel capacity for the STBC MIMO system using D-dimensional M-ary signaling over the DCMC can be derived from that of the discrete memoryless channel (DMC) [24] as

$$C^{\text{STBC}}_{\text{DCMC}} = \max_{p(\mathbf{x}_1),\ldots,p(\mathbf{x}_M)} \sum_{m=1}^{M} \underbrace{\int_{-\infty}^{\infty} \cdots \int_{-\infty}^{\infty}}_{\text{D-fold}} p(\vec{\mathbf{y}}|\mathbf{x}_m)p(\mathbf{x}_m) \cdot \log_2 \left(\frac{p(\vec{\mathbf{y}}|\mathbf{x}_m)}{\sum_{n=1}^{M} p(\vec{\mathbf{y}}|\mathbf{x}_n)p(\mathbf{x}_n)} \right) d\vec{\mathbf{y}} \quad \text{[bit/sym]} \tag{8}$$

where $p(\mathbf{x}_m)$ is the probability of occurrence for the transmitted signal $\mathbf{x}_m$. It was shown in [24, p. 94] that for a symmetric DMC, the full capacity may only be achieved by using equiprobable inputs. Hence, the right-hand side of (8) is maximized when the transmitted symbols are equiprobably distributed, i.e., when we have $p(\mathbf{x}_m) = 1/M$ for $m \in \{1, \ldots, M\}$. Hence, we arrive at

$$\begin{aligned} &\log_2 \left(\frac{p(\vec{\mathbf{y}}|\mathbf{x}_m)}{\sum_{n=1}^{M} p(\vec{\mathbf{y}}|\mathbf{x}_n)p(\mathbf{x}_n)} \right) \\ &\quad = -\log_2 \left(\frac{1}{M} \sum_{n=1}^{M} \frac{p(\vec{\mathbf{y}}|\mathbf{x}_n)}{p(\vec{\mathbf{y}}|\mathbf{x}_m)} \right) \\ &\quad = \log_2(M) - \log_2 \sum_{n=1}^{M} \exp(\Psi_{m,n}) \end{aligned} \tag{9}$$

where the term $\Psi_{m,n}$ is given by

$$\begin{aligned} &\Psi_{m,n} \\ &\quad = \sum_{d=1}^{D} \sum_{i=1}^{N_r} \left(\frac{-\left(y_i[d] - \chi^2_{2N_t,i}[d]x_n[d]\right)^2}{\chi^2_{2N_t,i}[d]N_0} + \frac{\left(y_i[d] - \chi^2_{2N_t,i}[d]x_m[d]\right)^2}{\chi^2_{2N_t,i}[d]N_0} \right) \\ &\quad = \sum_{d=1}^{D} \sum_{i=1}^{N_r} \left(\frac{\left(\chi^2_{2N_t,i}[d]\,(x_m[d] - x_n[d]) + \Omega_i[d]\right)^2}{\chi^2_{2N_t,i}[d]N_0} + \frac{(\Omega_i[d])^2}{\chi^2_{2N_t,i}[d]N_0} \right). \end{aligned} \tag{10}$$

By substituting (9) and $p(\mathbf{x}_m) = 1/M$ into (8), we have

$$
\begin{aligned}
&C_{\mathrm{DCMC}}^{\mathrm{STBC}} \\
&= \frac{\log_2(M)}{M} \sum_{m=1}^{M} \underbrace{\int_{-\infty}^{\infty} \cdots \int_{-\infty}^{\infty}}_{\mathrm{D-fold}} p(\vec{\mathbf{y}}|\mathbf{x}_m)\, d\vec{\mathbf{y}} \\
&\quad - \frac{1}{M} \sum_{m=1}^{M} \underbrace{\int_{-\infty}^{\infty} \cdots \int_{-\infty}^{\infty}}_{\mathrm{D-fold}} p(\vec{\mathbf{y}}|\mathbf{x}_m) \log_2 \sum_{n=1}^{M} \exp(\Psi_{m,n})\, d\vec{\mathbf{y}} \\
&= \log_2(M) - \frac{1}{M} \sum_{m=1}^{M} E\left[\log_2 \sum_{n=1}^{M} \exp(\Psi_{m,n}) \middle| \mathbf{x}_m \right] \text{[bit/sym]}
\end{aligned}
\tag{11}
$$

where $E[A|\mathbf{x}_m]$ is the expectation of A conditioned on $\mathbf{x}_m$, and the expectation in (11) is taken over $\chi^2_{2N_t,i}[d]$ and $\Omega_i[d]$ for $i = \{1, \ldots, N_r\}$. This expected value can be estimated using the Monte Carlo averaging method. More specifically, (11) represents the capacity of the MIMO DCMC when employing STBC for achieving full diversity gain for D-dimensional M-ary PSK/QAM signals with the aid of N_t number of transmit antennas and N_r number of receive antennas.

Note that, in an SISO AWGN channel, we have $\chi^2_{2N_t,i}[d] = N_t = 1$, and, hence, the noise variance of $\Omega_i[d]$ is $N_0/2$ for every dimension. For $D =$ 2-D signaling, (10) can be simplified to $\Psi_{m,n} = \sum_{i=1}^{N_r}((-|\chi^2_{2N_t,i}(\mathbf{x}_m - \mathbf{x}_n) + \Omega_i|^2 + |\Omega_i|^2)/\chi^2_{2N_t,i}N_0)$, where we have $\mathbf{x}_k = x_k[1] + jx_k[2]$ and $\mathbf{\Omega}_i = \Omega_i[1] + j\Omega_i[2]$. It is reassuring to note that, in the simplified case of SISO AWGN channels, (10) and (11) agree with the results of [25]. The average signal-to-noise ratio (SNR) can be determined from [16], [25] as

$$
\mathrm{SNR} = \frac{\frac{1}{M}\sum_{m=1}^{M}\sum_{d=1}^{D}|x_m[d]|^2}{\sum_{d=1}^{D} E\left[(\Omega_i[d])^2\right]} = \frac{E_s}{\frac{DN_0}{2}} \tag{12}
$$

where E_s is the average energy of the D-dimensional M-ary symbol $\mathbf{x}_m$ and $D(N_0/2)$ is the average energy of the D-dimensional AWGN. Additionally, the energy of the signal sets is further normalized by $\sqrt{N_t}$. More specifically, we have $x_k[d] = \tilde{x}_k[d]/\sqrt{N_t}$, where $\tilde{x}_k[d]$ is the kth modulated signal for $k = \{1, \ldots, M\}$ of dimension d in the case of $N_t = 1$. In an AWGN channel, the channel capacity is not expected to increase when N_t is increased. However, if the transmitter knows the complex Rayleigh-distributed channel coefficient of each of the MIMO links, the transmitted power to be assigned to the various transmit antennas can be distributed according to the "water-filling" principle [12], [15] in order to increase the achievable capacity.

The capacity formula of (10) and (11) can also be applied to real-valued signal sets, such as M-ary orthogonal signals, as well as to amplitude-modulated signals following straightforward adjustments of the signaling space dimensionality, the channel fading, and the noise. The MIMO CCMC capacity (unrestricted bound) of the STBC scheme designed for achieving full diversity gain can be derived based on the equivalent SIMO channel of (4) as

$$
\begin{aligned}
&C_{\mathrm{CCMC}}^{\mathrm{STBC}} \\
&\quad = E\left[WT \log_2\left(1 + \sum_{i=1}^{N_r} \chi^2_{2N_t,i} \frac{\mathrm{SNR}}{N_t}\right)\right] \text{ [bit/sym]} \\
&\quad = E\left[\frac{D}{2} \log_2\left(1 + \chi^2_{2N} \frac{\mathrm{SNR}}{N_t}\right)\right] \text{ [bit/sym]}
\end{aligned}
\tag{13}
$$

where $\chi^2_{2N} = \sum_{i=1}^{N_r} \chi^2_{2N_t,i} = \sum_{i=1}^{N_r}\sum_{j=1}^{N_t} |\mathbf{h}_{i,j}|^2$, and the expectation is taken over χ^2_{2N}. Again, the achievable capacity can be further enhanced by distributing the transmitted power according to the "water-filling" principle when the channel knowledge is available at the transmitter [12], [15].

IV. General MIMO Channel Capacity

In a 2-D MIMO system, there are $M = L^{N_t}$ number of possible L-ary PSK/QAM phasor combinations in the transmitted signal vector $\vec{\mathbf{x}} = (\mathbf{x}_1, \ldots, \mathbf{x}_{N_t})^T$, where $\mathbf{x}_j$ is the 2-D L-ary PSK/QAM signal emitted from antenna j. The STTC scheme of [5], which is designed for attaining transmit diversity and coding gain, may be viewed as a rate-$1/N_t$ channel code, where there are only $L^1 = L$ legitimate space–time code words out of the L^{N_t} possible phasor combinations during each transmission period. By contrast, the BLAST scheme [7] designed for attaining multiplexing gain may be viewed as a rate-1 channel code, where all L^{N_t} phasor combinations are legitimate during each transmission period. In the case of the SISO system, the higher the temporal diversity (coding gain), the lower the coding rate; hence, a lower throughput is derived. Similarly, in the case of the MIMO system, the higher the transmit diversity (a maximum of order N_t), the lower the coding rate (multiplexing gain); hence, a lower throughput is obtained.

Let us consider a general MIMO system that invokes N_t transmit antennas and N_r transmit antennas. We will refer to this general MIMO system as the ML-detected MIMO system for the sake of differentiating it from the orthogonal STBC-based MIMO system discussed in Section III. When $D =$ 2-D L-ary PSK/QAM is employed, the received signal vector of the MIMO system is given by

$$
\vec{\mathbf{y}} = \mathbf{H}\vec{\mathbf{x}} + \vec{\mathbf{n}} \tag{14}
$$

where $\vec{\mathbf{y}} = (\mathbf{y}_1, \ldots, \mathbf{y}_{N_r})^T$ is an N_r-element vector of the received signals, $\mathbf{H}$ is an $N_r \times N_t$ channel matrix, $\vec{\mathbf{x}} = (\mathbf{x}_1, \ldots, \mathbf{x}_{N_t})^T$ is an N_t-element vector of the transmitted signals, and $\vec{\mathbf{n}} = (\mathbf{n}_1, \ldots, \mathbf{n}_{N_r})^T$ is an N_r-element noise vector, where each element in $\vec{\mathbf{n}}$ is an AWGN having a zero mean and a variance of $N_0/2$ per dimension. The 2-D-signaling-based (14) can be generalized for $D = 2V$-dimensional signals as

$$
\vec{\mathbf{y}}[v] = \mathbf{H}[v]\vec{\mathbf{x}}[v] + \vec{\mathbf{n}}[v] \tag{15}
$$

where $\vec{\mathbf{Y}} = (\vec{\mathbf{y}}[1], \ldots, \vec{\mathbf{y}}[V])$ is defined as the $2V$-dimensional received signal vector, $\vec{\mathbf{X}} = (\vec{\mathbf{x}}[1], \ldots, \vec{\mathbf{x}}[V])$ is defined as the $2V$-dimensional transmitted signal vector, $\mathbf{H}[v]$ is the vth

element of the $2V$-dimensional channel matrix, and $\vec{\mathbf{n}}[v]$ is the vth element of the $2V$-dimensional AWGN vector. As we have seen in Fig. 1, there are $(V-1)$ number of subsets that are orthogonal to a particular subset in $2V$-dimensional L-orthogonal PSK/QAM signaling. There are a total of V^{N_t} number of possible transmitted phasor constellation combinations in the $2V$-dimensional L-orthogonal PSK/QAM signaling. However, from the V^{N_t} number of constellation combinations, only $(V-1)$ are orthogonal to a particular phasor constellation, because the dimensionality is still $D=2V$.

To elaborate a little further, let us define a set of basis functions $\vec{\Phi}_k$ that are not necessarily orthogonal to each other for representing the V^{N_t} possible transmitted phasor constellation combinations for $k \in \{1,\ldots,V^{N_t}\}$. More specifically, the aforementioned basis function $\vec{\Phi}_k$ may be described by an $N_t \times V$ matrix that can be constructed from nonoverlapping signaling pulses for each of the rows, where there is only a single "1" in each of the N_t rows. Explicitly, we have $\vec{\Phi}_k = (\vec{\phi}_k[1],\ldots,\vec{\phi}_k[v],\ldots,\vec{\phi}_k[V])$, where $\vec{\phi}_k[v] = (\phi_{k,1}[v],\ldots,\phi_{k,j}[v],\ldots,\phi_{k,N_t}[v])^T$ is an N_t-element column vector and $\phi_{k,j}[v] \in \{0,1\}$. The relationship between the transmitted N_t-element vector $\vec{\mathbf{x}}[v]$, the L-ary PSK/QAM signal $\mathbf{x}_j^L$ transmitted from the jth transmit antenna, and the vth column vector of the basis function $\vec{\phi}_k[v]$ may be formulated as

$$\begin{aligned}\vec{\mathbf{x}}[v] &= \vec{\mathbf{x}}^L \cdot \vec{\phi}_k[v] \\ &= \left(\mathbf{x}_1^L \phi_{k,1}[v],\ldots,\mathbf{x}_j^L \phi_{k,j}[v],\ldots,\mathbf{x}_{N_t}^L \phi_{k,N_t}[v]\right)^T \end{aligned} \quad (16)$$

where $\vec{\mathbf{x}}^L = (\mathbf{x}_1^L,\ldots,\mathbf{x}_j^L,\ldots,\mathbf{x}_{N_t}^L)^T$ is the N_t-element column vector representing the N_t L-ary PSK/QAM phasors transmitted from N_t transmitters. Again, there are V^{N_t} transmitted phasor constellation combinations in a general MIMO system, and each constellation combination can host L^{N_t} number of L-ary PSK/QAM phasor combinations. Hence, the total number of possible combinations for $\vec{\mathbf{X}}$ is given by

$$M = (VL)^{N_t}. \quad (17)$$

Fig. 2 portrays the $V^{N_t} = 2^2 = 4$ legitimate phasor constellation combinations for the $N_t = 2$ MIMO $D = 2V = 4$-dimensional L-orthogonal PSK/QAM signaling scheme. As shown in Fig. 2, we can always find $(V-1)=1$ orthogonal phasor constellation combination for each of the $V^{N_t}=4$ possible phasor constellation combination. In other words, the vectors $(\vec{\Phi}_1,\vec{\Phi}_2)$ and $(\vec{\Phi}_4,\vec{\Phi}_3)$ constitute the $V=2$ orthogonal basis functions for this system.

The conditional probability of receiving a $2V$-dimensional signal vector $\vec{\mathbf{Y}}$ given that a $2V$-dimensional M-ary signal vector $\vec{\mathbf{X}}_m$ for $m \in \{1,\ldots,M\}$ was transmitted over Rayleigh-fading channels is determined by the PDF of the noise, which yields

$$\begin{aligned} p\left(\vec{\mathbf{Y}}|\vec{\mathbf{X}}_m\right) &= \prod_{v=1}^{V} \frac{1}{\pi N_0} \exp\left(\frac{-\|\vec{\mathbf{y}}[v] - \mathbf{H}[v]\vec{\mathbf{x}}_m[v]\|^2}{N_0}\right) \\ &= \frac{1}{(\pi N_0)^V} \exp\left(\sum_{v=1}^{V} \frac{-\|\vec{\mathbf{y}}[v] - \mathbf{H}[v]\vec{\mathbf{x}}_m[v]\|^2}{N_0}\right). \end{aligned} \quad (18)$$

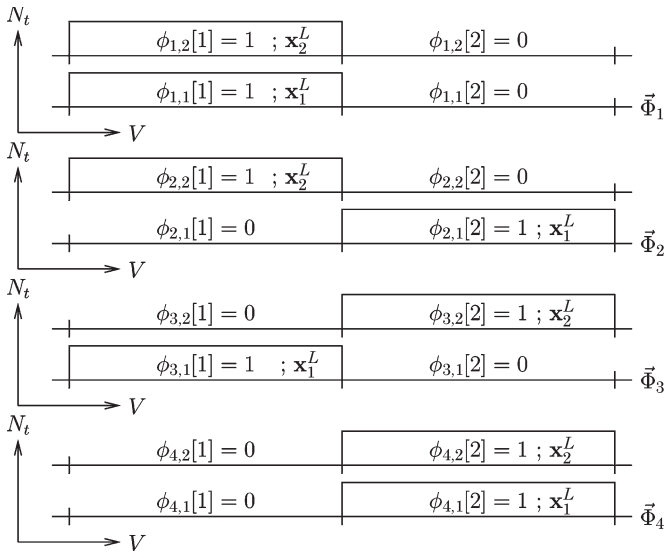

Fig. 2. $V^{N_t}=4$ phasor constellation combinations for the $D=2V=4$-dimensional $N_t=2$ ML-detected L-orthogonal PSK/QAM signaling scheme.

The channel capacity of the ML-detected MIMO system using $2V$-dimensional M-ary signaling over the DCMC can be written as

$$\begin{aligned} C_{\text{DCMC}}^{\text{ML}} = \max_{p(\vec{\mathbf{X}}_1),\ldots,p(\vec{\mathbf{X}}_M)} \sum_{m=1}^{M} \underbrace{\int_{-\infty}^{\infty} \cdots \int_{-\infty}^{\infty}}_{\text{V-fold}} p(\vec{\mathbf{Y}}|\vec{\mathbf{X}}_m) p(\vec{\mathbf{X}}_m) \\ \cdot \log_2\left(\frac{p(\vec{\mathbf{Y}}|\vec{\mathbf{X}}_m)}{\sum_{n=1}^{M} p(\vec{\mathbf{Y}}|\vec{\mathbf{X}}_n) p(\vec{\mathbf{X}}_n)}\right) d\vec{\mathbf{Y}} \quad \text{[bit/sym]} \end{aligned} \quad (19)$$

where the right-hand side of (19) is maximized when we have $p(\vec{\mathbf{X}}_m) = 1/M$ for $m \in \{1,\ldots,M\}$. Hence, (19) can be simplified as

$$C_{\text{DCMC}}^{\text{ML}} = \log_2(M) - \frac{1}{M}\sum_{m=1}^{M} E\left[\log_2 \sum_{n=1}^{M} \exp(\Psi_{m,n}) \middle| \vec{\mathbf{X}}_m\right] \quad \text{[bit/sym]} \quad (20)$$

where $E[A|\vec{\mathbf{X}}_m]$ is the expectation of A conditioned on $\vec{\mathbf{X}}_m$, and the expectation in (20) is taken over $\mathbf{H}[v]$ and $\vec{\mathbf{n}}[v]$, whereas $\Psi_{m,n}$ is given by

$$\begin{aligned} \Psi_{m,n} &= \sum_{v=1}^{V} \frac{-\|\mathbf{H}[v]\left(\vec{\mathbf{x}}_m[v] - \vec{\mathbf{x}}_n[v]\right) + \vec{\mathbf{n}}[v]\|^2 + \|\vec{\mathbf{n}}[v]\|^2}{N_0} \\ &= \sum_{v=1}^{V}\sum_{i=1}^{N_r} \frac{-\left|\vec{\mathbf{h}}_i[v]\left(\vec{\mathbf{x}}_m[v] - \vec{\mathbf{x}}_n[v]\right) + \mathbf{n}_i[v]\right|^2 + |\mathbf{n}_i[v]|^2}{N_0} \end{aligned} \quad (21)$$

where $\vec{\mathbf{h}}_i[v]$ is the ith row of $\mathbf{H}[v]$, and $\mathbf{n}_i[v]$ is the AWGN at the ith receiver.

It was shown in [12] and [15] that the MIMO capacity of the CCMC can be expressed as

$$C_{\mathrm{CCMC}}^{\mathrm{ML}} = E\left[WT\sum_{i=1}^{r}\log_2\left(1+\lambda_i\frac{\mathrm{SNR}}{N_t}\right)\right] \qquad (22)$$

where r is the rank of $\mathbf{Q}$, which is defined as $\mathbf{Q}=\mathbf{H}^H\mathbf{H}$ for $N_r \geq N_t$ or $\mathbf{Q}=\mathbf{H}\mathbf{H}^H$ for $N_r < N_t$. Furthermore, λ_i is the ith eigenvalue of the matrix $\mathbf{Q}$. The extension of (22) to D-dimensional signaling can be carried out by noting that $WT = D/2 = V$.

When communicating over AWGN channels and assuming that there is no path loss, we have $\mathbf{h}_{i,j}=1$ for all i and j in the channel matrix $\mathbf{H}$. Hence, the rank of $\mathbf{Q}$ becomes unity, and the only zero eigenvalue is given by $\lambda_1 = N_r \times N_t$ [15]. The capacity of the AWGN CCMC becomes identical to that of the orthogonal STBC scenario characterized in (13), where $\chi^2_{2N}/N_t = N_r$. Therefore, no multiplexing or transmit diversity gain may be attained in an AWGN CCMC. On the other hand, we have $\mathbf{H}\vec{\mathbf{x}} = N_r\sum_{j=1}^{N_t}\mathbf{x}_j$ when communicating over an AWGN DCMC. More explicitly, the signals transmitted from the N_t transmit antennas may cancel out each other and result in a severe interference. Hence, no multiplexing or transmit diversity gain may be attained in the AWGN DCMC, and its capacity is also the same as that of the orthogonal STBC scheme quantified by (10) and (11), where $\chi^2_{2N_t,i}[d] = N_t$.

Note that the closed-form evaluation of the MIMO CCMC capacity in (22) has been given in [13, eq. (40)] and [14]. A closed-form evaluation of the channel capacity for the MIMO CCMC when employing STBC in (13) may also be derived based on [13] and [14]. However, a closed-form evaluation of the MIMO DCMC channel capacity in (11) and (19) is computationally complex because of the existence of the "summation over M exponential functions" in the multidimensional integral. In this case, the Monte Carlo averaging method is the most efficient approximation technique of computing the expectation terms.

V. Numerical Results

In this section, we will evaluate both the capacity and the bandwidth efficiency of MIMO channels for the scenario when the transmitter does not have any channel knowledge. Explicitly, the bandwidth efficiency is computed by normalizing the channel capacity as it transpires from (11), (13), (19), and (22) with respect to the product of the bandwidth W and the signaling period T, which is written as

$$\eta = \frac{C}{WT} = \frac{C}{\frac{D}{2}} \quad [\mathrm{bit/s/Hz}]. \qquad (23)$$

The bandwidth efficiency is typically plotted against the SNR per bit given by $E_b/N_0 = \mathrm{SNR}/\eta$. We denote the "$L=16$-orthogonal QAM scheme having $V=v$" as "16QAM, $V=v$" for brevity. Again, $L=16$-orthogonal PSK/QAM signaling having $V=1$ represents classic 2-D L-ary PSK/QAM signaling.

Fig. 3 illustrates the achievable capacity C of both the uncorrelated MIMO Rayleigh-fading channel and the AWGN channel for 16QAM signaling having both $V=1$ and $V=2$ when aiming for a full diversity gain using an orthogonal STBC scheme. As shown in Fig. 3, the achievable capacity of the Rayleigh-fading channel increases as the number of transmit antennas N_t increases from 1 to 4, approaching the capacity of the AWGN channel, which is independent of N_t. Fig. 4 depicts the bandwidth efficiency η of both the uncorrelated MIMO Rayleigh-fading channel and the AWGN channel for 16QAM signaling having both $V=1$ and $V=2$ when aiming for a full diversity gain using an orthogonal STBC scheme. It is shown in Fig. 4 that as N_r increases, the bandwidth efficiency of the AWGN channel also improves. Hence, the corresponding performance over Rayleigh-fading channels follows the same trend. However, the attainable extra transmit diversity gain of the Rayleigh-fading channel reduces as N_r increases, because a near-AWGN performance is achieved by the high-order receiver diversity. As seen by comparing Figs. 3 and 4 for the systems having $N_r = 1$, the achievable channel capacity increases as the signal dimensionality D increases, although this is attained at a reduced bandwidth efficiency. However,

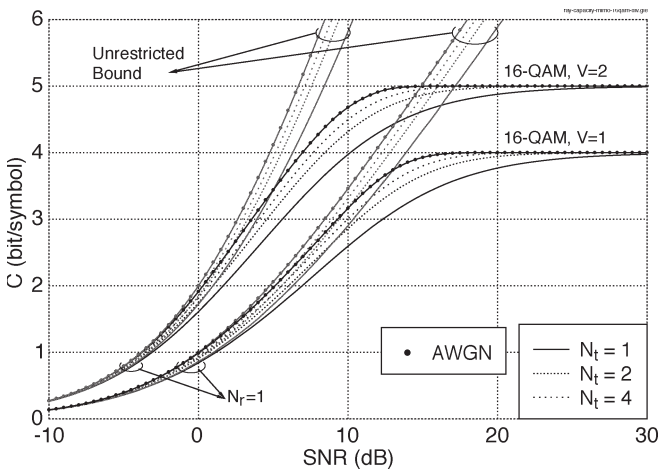

Fig. 3. Capacity of the orthogonal STBC MIMO uncorrelated Rayleigh-fading channel and AWGN channel for 16QAM having $V=1$ ($M=16$ and $D=2$) and $V=2$ ($M=32$ and $D=4$).

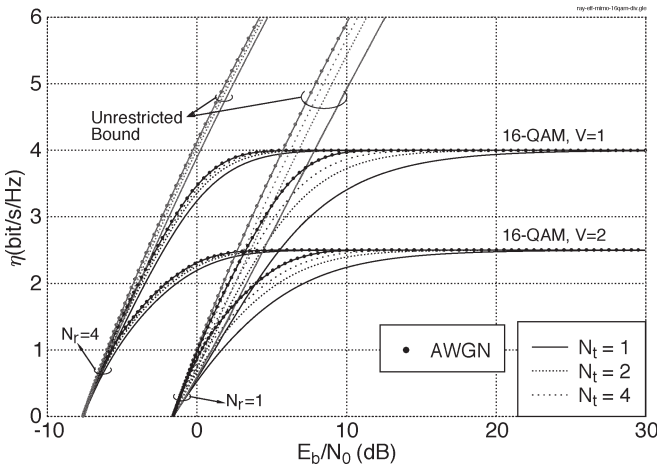

Fig. 4. Bandwidth efficiency of the orthogonal STBC MIMO uncorrelated Rayleigh-fading channel and AWGN channel for 16QAM having $V=1$ ($M=16$ and $D=2$) and $V=2$ ($M=32$ and $D=4$).

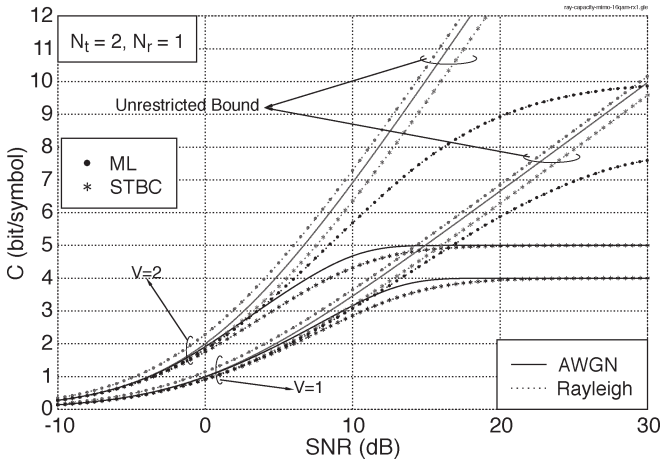

Fig. 5. Capacity of the MIMO uncorrelated Rayleigh-fading channel and AWGN channel for 16QAM having $V = 1$ ($M = 16$ and $D = 2$) and $V = 2$ ($M = 32$ and $D = 4$) when $N_r = 1$.

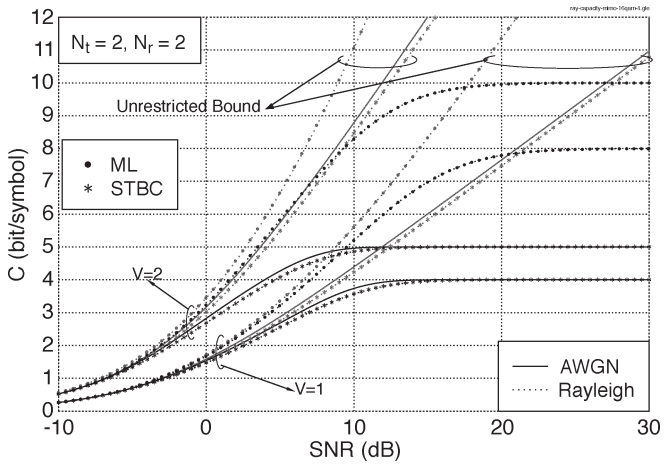

Fig. 6. Capacity of the MIMO uncorrelated Rayleigh-fading channel and AWGN channel for 16QAM having $V = 1$ ($M = 16$ and $D = 2$) and $V = 2$ ($M = 32$ and $D = 4$) when $N_r = 2$.

the error resilience of the power-efficient multidimensional orthogonal signals also improves as the dimensionality increases [3]. As evidenced in Fig. 4, at low E_b/N_0, the bandwidth efficiency η of 16QAM attained in conjunction with both $V = 1$ and $V = 2$ converges to the unrestricted bound. Note that the unrestricted bound is independent of the signal dimensionality.

Let us now compare the achievable capacity of the orthogonal STBC MIMO system to that of the general (ML detected) MIMO system in Figs. 5 and 6, where the number of receivers is $N_r = 1$ and $N_r = 2$, respectively. As we can see in Fig. 5, the Rayleigh-fading CCMC capacity (unrestricted bound) of the ML-detected MIMO system is higher than that of the orthogonal STBC system by a constant margin when we have $N_r = 1$ and $N_t = 2$. However, the Rayleigh-fading DCMC capacity of the ML-detected MIMO system is identical to that of the orthogonal STBC system when the channel SNR is low. When the number of receivers is increased to $N_r = 2$, the gap between the Rayleigh-fading CCMC/DCMC capacity of the ML-detected MIMO system and that of the orthogonal STBC system increases as the SNR increases, which is depicted in Fig. 6. Hence, the capacity loss of the orthogonal STBC MIMO system increases as N_r and the SNR increase. However, the ML-detected MIMO system, which has $(VL)^{N_t}$ possible transmitted signals, imposes a higher detection complexity compared to that of the orthogonal STBC system, which has only VL number of possible transmitted signals. Hence, it is more beneficial to employ the orthogonal STBC system when invoking a low-rate channel coding scheme, which results in a low throughput, because a lower detection complexity is required compared to that of the ML-detected MIMO system, especially when we have $N_r = 1$. By contrast, a higher capacity can be attained with the aid of the ML-detected MIMO system at the cost of a higher complexity and a higher SNR.

Let us now compare the Rayleigh-fading MIMO channel capacity of the STBC, STTC, and BLAST MIMO schemes at $N_t = N_r = 2$ and $V = 1$ in Fig. 6. At a throughput of $C = 4$ b/symbol , the required SNRs for the STTC/BLAST and the STBC schemes are approximately 7.0 dB $(E_b/N_0 = 1$ dB) and 14.5 dB $(E_b/N_0 = 8.5$ dB), respectively. Inasmuch as both the STBC and the STTC schemes achieve a full transmit diversity gain, the gap between the capacity curves of STBC and STTC quantifies the attainable temporal diversity gain (or coding gain) for the STTC scheme. Hence, the STTC scheme is capable of achieving an additional coding gain of 7.5 dB compared to the STBC scheme at a throughput of 4 b/symbol. Similarly, with the aid of a rate $R_o = 1/2$ outer channel code, the BLAST scheme is capable of benefiting from the coding gain of the outer channel code and, hence, achieve a similar performance to the STTC scheme at a throughput of $8R_o = 4$ b/symbol. However, the BLAST scheme by itself requires an SNR of approximately 27.0 dB (or $E_b/N_0 = 18.0$ dB) in order to achieve a full multiplexing gain of 8 b/symbol. Hence, when aiming for a near–error-free performance, the BLAST scheme, which exhibits a full transmit multiplexing gain, is $18.0 - 8.5 = 9.5$ dB inferior in terms of the required E_b/N_0 compared to the orthogonal STBC scheme, which exhibits a full transmit diversity gain. In other words, the full spatial diversity offers an achievable gain of 9.5 dB in this MIMO system. Furthermore, the BLAST scheme is $18.0 - 1.0 = 17.0$ dB inferior in terms of the required E_b/N_0 compared to the STTC scheme, which exhibits a full transmit diversity gain plus a coding gain. Hence, a total of 17.0 dB E_b/N_0 reduction was offered by the spatial and temporal diversity. In the same way, the tradeoffs associated with having partial transmit multiplexing and transmit diversity gain may also be quantified based on the corresponding MIMO DCMC channel capacity curves. Note further that the capacity of the Rayleigh-fading MIMO channel of the ML-detected system is higher than that of the AWGN MIMO channel. However, the capacity of the Rayleigh-fading MIMO channel of the orthogonal STBC system is lower than that of the AWGN MIMO channel.

The asymptotic capacity of a DCMC system is given by $\log_2(M)$ b/symbol, where we have $M = (VL)^{N_t}$ for an ML-detected MIMO system and $M = VL$ for an orthogonal STBC system. Hence, a variety of different systems may be designed for achieving a given M by changing the values of V, L, and N_t. As we can see in Fig. 7, where we have $M = 256$ for all schemes, the different system designs achieve different performance, despite having the same asymptotic capacity of

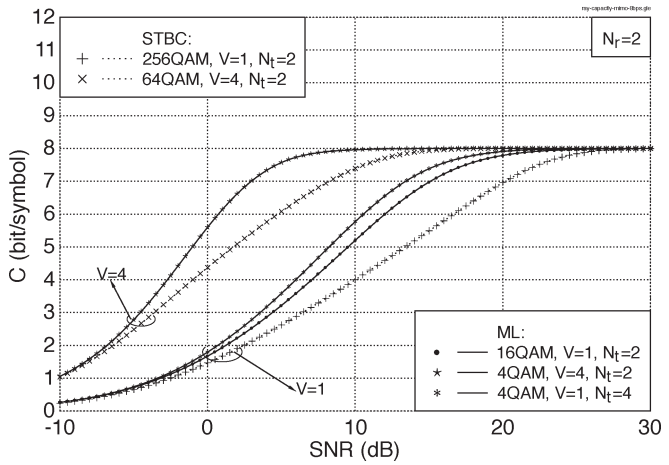

Fig. 7. Capacity of the MIMO uncorrelated Rayleigh-fading channel for $D = 2$ $(V = 1)$ and $D = 8$ $(V = 4)$-dimensional signaling when aiming for a throughput of 8 b/symbol.

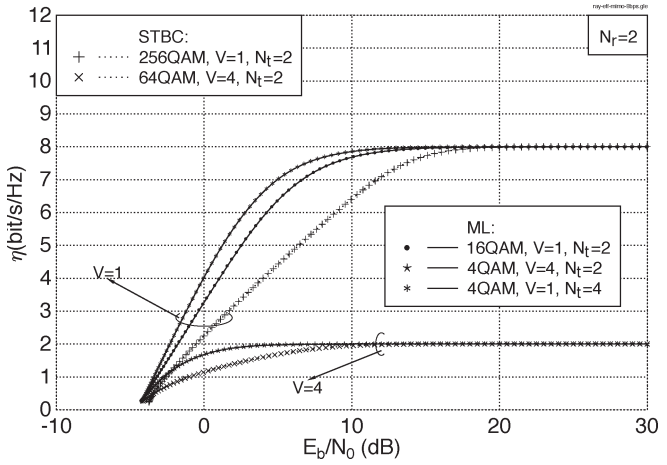

Fig. 8. Bandwidth efficiency of the MIMO uncorrelated Rayleigh-fading channel for $D = 2$ $(V = 1)$ and $D = 8$ $(V = 4)$-dimensional signaling when aiming for a throughput of 8 b/symbol.

8 b/symbol. Again, neither the BLAST nor the STBC scheme achieves a coding gain, unless an outer code is employed. However, for achieving the same asymptotic capacity using $V = 1$, the full-diversity-based orthogonal STBC MIMO system has to employ the higher order modulation scheme of 256QAM compared to the 16QAM arrangement used by the BLAST scheme. As can be seen in Fig. 7, the full-diversity advantage of STBC cannot compensate for the minimum Euclidean distance loss imposed by employing 256QAM. This observation is also applicable for higher dimensionality signaling, where the BLAST MIMO system having $L = 4$ and $V = 4$ performs better than the orthogonal STBC system having $L = 64$ and $V = 4$. In the context of the ML-detected MIMO system, a scheme that employs a lower L and a higher N_t ($L = 4$, $N_t = 4$, $V = 1$) may yield a higher capacity compared to a scheme that invokes a higher L and a lower N_t ($L = 16$, $N_t = 2$, $V = 1$) when aiming for the same M, albeit this is achieved at the cost of a higher hardware complexity. When the signal dimensionality is increased from two $(V = 1)$ to eight $(V = 4)$, the achievable capacity also increases at the cost of a higher bandwidth requirement. The bandwidth efficiency of the $M = 256$-based schemes characterized in Fig. 7 is shown in Fig. 8. As we can see in Fig. 8, the bandwidth efficiency of the eight-dimensional scheme is poorer than that of the 2-D scheme. The performance difference between the ML-detected MIMO system and the orthogonal STBC system is also more apparent in terms of their bandwidth efficiency. Again, the ML-detected scheme having $L = 4$, $N_t = 4$, and $V = 1$ is more bandwidth efficient than the ML-detected arrangement having $L = 16$, $N_t = 2$, and $V = 1$.

VI. Conclusion

The capacity formulas of DCMC were derived for a specific orthogonal STBC MIMO system and for a general MIMO system when employing multidimensional signal sets. The orthogonal STBC MIMO system was found to have a lower capacity, because its code orthogonality prevents it from achieving temporal diversity. Furthermore, STTC is a specific MIMO system that attains full transmit diversity and a coding gain, whereas BLAST is a specific MIMO system that achieves only the full transmit multiplexing gain. It was shown that transmit diversity is capable of narrowing the gap between the capacity of the Rayleigh-fading channel and that of the AWGN channel. However, the transmit diversity advantage becomes modest when the receiver diversity order is increased, because the remaining capacity gap becomes narrower. Hence, it is better to utilize temporal diversity for enhancing error resilience while employing multiple transmitters for attaining transmit multiplexing gain, when sufficient receiver diversity is achieved. When aiming for a similar asymptotic capacity, the highest bandwidth efficiency is attained when employing a 2-D ML-detected MIMO system having the lowest L and the highest N_t at the cost of a higher hardware complexity. By contrast, the highest capacity was achieved at a given asymptotic capacity when an ML-detected MIMO system having the highest dimensions, a low L, and a high N_t was employed, although this was achieved at the cost of a higher bandwidth requirement.

Acknowledgment

The authors are grateful to Dr. J. Kliewer for his insightful comments that helped in improving the presentation of this paper.

References

[1] C. E. Shannon, "A mathematical theory of communication," *Bell Syst. Tech. J.*, vol. 27, no. 3, pp. 379–423, Jun. 1948.

[2] ——, "A mathematical theory of communication," *Bell Syst. Tech. J.*, vol. 27, no. 4, pp. 623–656, Oct. 1948.

[3] J. G. Proakis, *Digital Communications*, 3rd ed. New York: McGraw-Hill, 1995.

[4] L. Hanzo, S. X. Ng, W. Webb, and T. Keller, *Quadrature Amplitude Modulation: From Basics to Adaptive Trellis-Coded, Turbo-Equalised and Space–Time Coded OFDM, CDMA and MC–CDMA Systems*. New York: Wiley, 2004.

[5] V. Tarokh, N. Seshadri, and A. R. Calderbank, "Space–time codes for high rate wireless communication: Performance analysis and code construction," *IEEE Trans. Inf. Theory*, vol. 44, no. 2, pp. 744–765, Mar. 1998.

[6] S. M. Alamouti, "A simple transmitter diversity scheme for wireless communications," *IEEE J. Sel. Areas Commun.*, vol. 16, no. 8, pp. 1451–1458, Oct. 1998.
[7] G. J. Foschini, Jr., "Layered space–time architecture for wireless communication in a fading environment when using multi-element antennas," *Bell Labs Tech. J.*, vol. 1, no. 2, pp. 41–59, 1996.
[8] L. Zheng and D. Tse, "Diversity and multiplexing: A fundamental tradeoff in multiple antenna channels," *IEEE Trans. Inf. Theory*, vol. 49, no. 5, pp. 1073–1096, May 2003.
[9] V. Tarokh, H. Jafarkhani, and A. R. Calderbank, "Space–time block codes from orthogonal designs," *IEEE Trans. Inf. Theory*, vol. 45, no. 5, pp. 1456–1467, Jul. 1999.
[10] B. Hochwald, T. L. Marzetta, and C. B. Papadias, "A transmitter diversity scheme for wideband CDMA system based on space–time spreading," *IEEE J. Sel. Areas Commun.*, vol. 19, no. 1, pp. 48–60, Jan. 2001.
[11] G. Foschini, Jr. and M. Gans, "On limits of wireless communication in a fading environment when using multiple antennas," *Wireless Pers. Commun.*, vol. 6, no. 3, pp. 311–335, Mar. 1998.
[12] E. Telatar, "Capacity of multi-antenna Gaussian channels," *Eur. Trans. Telecommun.*, vol. 10, no. 6, pp. 585–595, Nov./Dec. 1999.
[13] M.-S. Alouini and A. J. Goldsmith, "Capacity of Rayleigh fading channels under different adaptive transmission and diversity-combining techniques," *IEEE Trans. Veh. Technol.*, vol. 48, no. 4, pp. 1165–1181, Jul. 1999.
[14] H. Shin and J. H. Lee, "Capacity of multiple-antenna fading channels: Spatial fading correlation, double scattering, and keyhole," *IEEE Trans. Inf. Theory*, vol. 49, no. 10, pp. 2636–2647, Oct. 2003.
[15] B. Vucetic and J. Yuan, *Space–Time Coding*. New York: Wiley, May 2003.
[16] P. E. McIllree, "Channel capacity calculations for M-ary N-dimensional signal sets," M.S. thesis, Sch. Electron. Eng., Univ. South Australia, Adelaide, Australia, 1995.
[17] W. C. Lindsey and M. K. Simon, "L-orthogonal signal transmission and detection," *IEEE Trans. Commun.*, vol. COMM-20, no. 5, pp. 953–960, Oct. 1972.
[18] I. S. Reed and R. A. Scholtz, "N-orthogonal phase modulated codes," *IEEE Trans. Inf. Theory*, vol. IT-12, no. 3, pp. 388–395, Jul. 1966.
[19] J. Wozencraft and I. Jacobs, *Principles of Communications Engineering*. New York: Wiley, 1965.
[20] G. D. Forney and L.-F. Wei, "Multidimensional constellations—Part I: Introduction, figures of merit, and generalized cross constellations," *IEEE J. Sel. Areas Commun.*, vol. 7, no. 6, pp. 877–892, Aug. 1989.
[21] L. Hanzo, L.-L. Yang, E.-L. Kuan, and K. Yen, *Single- and Multi-Carrier DS–CDMA: Multi-User Detection, Space–Time Spreading, Synchronisation and Standards*. New York: Wiley, 2003.
[22] S. X. Ng and L. Hanzo, "Space–time IQ-interleaved TCM and TTCM for AWGN and Rayleigh fading channels," *Electron. Lett.*, vol. 38, no. 24, pp. 1553–1555, Nov. 2002.
[23] L. He and H. Ge, "A new full-rate full-diversity orthogonal space–time block coding scheme," *IEEE Commun. Lett.*, vol. 7, no. 12, pp. 590–592, Dec. 2003.
[24] R. Gallager, *Information Theory and Reliable Communication*. New York: Wiley, 1968.
[25] G. Ungerböck, "Channel coding with multilevel/phase signals," *IEEE Trans. Inf. Theory*, vol. IT-28, no. 1, pp. 55–67, Jan. 1982.

Soon Xin Ng (M'03) received the B.Eng. degree in electronics engineering and the Ph.D. degree in mobile communications from the University of Southampton, Southampton, U.K., in July 1999 and December 2002, respectively.

He is currently continuing his research as a Postdoctoral Research Fellow at the University of Southampton. His research interests are mainly in adaptive coded modulation, channel coding, turbo coding, space–time coding, joint source and channel coding, and MIMO systems. He has published numerous papers in these fields.

Lajos Hanzo (M'91–SM'92–F'04) received the M.S. and Ph.D. degrees in electronics from the Technical University of Budapest, Budapest, Hungary, and the D.Sc. degree from the University of Southampton, Southampton, U.K., in 1976, 1983, and 2004, respectively.

During his 28-year career in telecommunications, he has held various research and academic posts in Hungary, Germany, and the U.K. Since 1986, he has been with the Department of Electronics and Computer Science, University of Southampton, where he holds the Chair in telecommunications. He is a nonexecutive Director of the Virtual Center of Excellence (VCE), Basingstoke, U.K., and an enthusiastic supporter of the industrial–academic liaison. He also offers a range of industrial research overview courses. He has coauthored 12 John Wiley/IEEE Press books on mobile radio communications, totaling about 9000 pages, published in excess of 600 research papers, organized and chaired conference sessions, and presented overview lectures. Further information on research in progress and associated publications may be found at http://www-mobile.ecs.soton.ac.uk.

Dr. Hanzo is Fellow of the Royal Academy of Engineering (FREng) and IEE. He is an IEEE Distinguished Lecturer of both the Communications Society and the Vehicular Technology Society. He has been awarded a number of distinctions. He is also the Governor of the IEEE Vehicular Technology Society and the Editor of the PROCEEDINGS OF THE IEEE.